VOL. 11, NO. 12, JUNE 2016 ISSN 1819-6608
ARPN Journal of Engineering and Applied Sciences

www.arpnjournals.com

IMPACT OF INJECTION ON A STAGNATION–POINT FLOW OF COPPER NANOFLUIDS OVER A VERTICAL POROUS SHRINKING OR STRETCHINGPLATE IN THE PRESENCE OF MAGNETIC FIELD

Ashwin Kumar E. N.[1], NorasikinBinti Mat Isa[1], VibhuVignesh B.[1] and Kandasamy R.[2]
[1]Faculty of Mechanical and Manufacturing Engineering, Malaysia
[2]Faculty of Science, Technology and Human Development, UniversitiTun Hussein Onn Malaysia, Johor, Malaysia

ABSTRACT

Nanofluids are the new generation way to enhance thermal properties of common fluids. The potential of nanofluidshave made them very useful in different heat transfer applications. In this paper, the injection velocity effects on copper nanofluids over permeable stretching/shrining surfaces are analysed in stagnation–point flow. Nanofluids are under the influence of magnetic field. The PDE governing the problem under consideration are transformed by similarity transformation into a system of ODE that is executed numerically using MAPLE 18 software. It is observed that the injection on magnetic field had greatly influenced the heat transfer characteristics in the copper nanofluid.

Keywords: coppernanofluids, stagnation-point flow, thermal radiation, magnetic field and heat source/sink.

INTRODUCTION

In recent years, numerous studies are performed on boundary layer flow of nanofluids over a stagnation-point flow. Nanofluid is a smart fluid, produced by properly dispersingnanometre-sized particles in conventional heat transfer basic fluids such as water, engine oil, etc., because these conventional heat transfer fluids have very heat transfer efficiency. In industries, these newly devolved smart fluids are extensively used. Studies on nanofluids elucidate that thermal conductivity enhances with increasing nanoparticles volume fraction. Therefore various methods have been made to increase the thermal conductivity of these fluids by suspending nano/micro sized particle materials in liquid. Choi (1995) developed these smart fluids and named them as nanofluids. Eastman, *et al.* (2001) proved that 1% volume concentration of nanoparticle in fluids can increase their thermal conductivity by two times. Wangand Mujumdar (2008) simulated the steady flow in a Newtonian fluid over a stretching hollow cylinder. The problem was governed by a high order non-linear ODE which led to appropriate similarity solutions of the Navier–Stokes equations. Khan andPop (2010) have simulated numerically the boundary layer flow of a nanofluid past a stretching surfaces.

Nazar *et al.* (2011) has investigated the stagnation-point flow of nanofluids over a shrinking surface. Ibrahimet al. (2013) have presented paper on stagnation-point flow and heat transfer of nanofluid towards a stretching surface under the influence of magnetic field. Hamad and Pop (2010) have analysed stagnation-point on a heated porous stretching surface saturated with a nanofluid and heat absorption/generation effects. The boundary layer flow of nanofluid influencing by magnetic field has numerous applications in engineering problems such as MHD generator, power generation in nuclear reactors, petroleum industries, power plants and Coal extraction. Considering the quality of operation process, radiative heat transfer in the boundary layer plays vital role in applications. Quality of process depends on the ambient fluid particles heat transfer rate. Usually nanofluid includes the effects of thermophoresis and Brownian motion. It was formulated by Buongiorno (2006). NieldandKuznetsov (2009) and Kuznetsov and Nield (2010) stated that nanofluids flow have affected by many physical factors but Brownian motion and thermophoresis plays vital role. Hamad and Ferdows (2011) investigated the boundary layer flow of electrically conducting fluid and heat transfer over a shrinking surface. They studied different types of nanoparticles and found each nanoparticle differs from others in physical characteristics each possess different character. They enclosed that changing the nanoparticle type, changes the behaviour of the fluid flow.

Mahapatra and Gupta (2001) observed the heat transfer in stagnation-point flow towards a stretching plate. The governing system of PDE was converted to ODE by using similarity transformations, then evaluated using the Keller-box method. The study was to understand the effects of the governing parameters, namely the suction/injection parameter, Prandtl number on the velocity and temperature profiles. MHD stagnation-point flow and boundary layer flow is studied by (Mahapatraand Gupta, 2002; Ishakand Nazar, 2008) over a stretching surface. According to their results, it is clear that when stretching velocity is lower than that of free stream velocity, there is an increase in velocity at one point with an increase in magnetic field.

The objective of the present work is to study the stagnation-point flow and heat transfer characteristic in Pal *et al.* (2014), permeable stretching/shrinking plate. In this paper, we investigate the behaviour of velocity and temperature profiles of copper nanofluids in the presence of magnetic field.

MATHEMATICAL ANALYSIS

The flow model for achieving our objectives is shown in Figure-1. In this study, the nanofluid flow

selected is a 2-D stagnation-point flow, over a permeable plate. The plate is subjected to shrinking and stretching and the flow is analysed in each plates. For stretching plate the linear velocity over a porous plate is $u_w = cx$ and the velocity over a porous plate becomes negative for shrinking plate that is $u_w = -cx$. The flow is time independent and laminar flow. $U(x) = ax$is defined as the free stream flow. Magnetic field strength (B_0) which is present in positive x-axis influences the nanofluid flow. Nanoparticles and base fluids are assumed to be in thermal equilibrium and no slip occurs between them. The acceleration due to gravity is denoted by g. The thermo-physical properties of base fluid and nanoparticle is given in Table 1. Prandtl number of water is taken as 6.2 at 20 ℃.

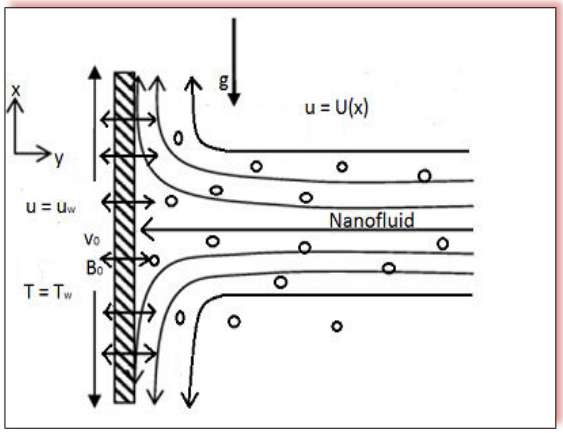

Figure-1. Stagnation-point flow model over a vertical permeable plate.

Table-1. Thermo-physical properties of fluid and copper nanoparticle. (Oztopand Abu-Nada, 2008).

Physical properties	Water	Cu
Cp(J/KgK)	4179	385
ρ(Kg/m^3)	997.1	8933
κ (W/mK)	0.613	401

With above assumptions, the boundary layer equations are as follows:

$$\frac{\partial u}{\partial x} + \frac{\partial v}{\partial y} = 0 \quad (1)$$

$$\left.\begin{aligned} u\frac{\partial u}{\partial x} + v\frac{\partial v}{\partial y} &= U(x)\frac{dU(x)}{dx} + \frac{\mu_{nf}}{\rho_{nf}}\frac{\partial^2 u}{\partial y^2} + \\ &\frac{\mu_{nf}}{\rho_{nf}K}(U(x) - u) \end{aligned}\right\} \quad (2)$$

$$\left.\begin{aligned} u\frac{\partial T}{\partial x} + v\frac{\partial T}{\partial y} &= \alpha_{nf}\frac{d^2T}{dy^2} + \frac{Q_0}{(\rho C_p)_{nf}}(T - T_\infty) - \\ &\frac{1}{(\rho C_p)_{nf}}\frac{\partial q_r}{\partial y} + \frac{\mu_{nf}}{(\rho C_p)_{nf}}\left(\frac{\partial u}{\partial y}\right)^2 \end{aligned}\right\} \quad (3)$$

Subjected to the boundary conditions (for shrinking or stretching plate)

$$\left.\begin{aligned} v = v_0, u = u_w(x) = \pm cx, T = T_w \text{ at } y = 0; \\ T \to T_\infty, u \to U(x) = ax, C \to C_\infty \text{ as } y \to \infty \end{aligned}\right\} \quad (4)$$

For calculating density, thermal conductivity, dynamic viscosity, thermal diffusivity and heat capacitance of nanofluids the below mentioned equations are used.

$$\rho_{nf} = (1-\phi)\rho_f + \phi\rho_s \quad (5)$$

$$\kappa_{nf} = \kappa_f\left[\frac{\kappa_s + 2\kappa_f - 2\phi(\kappa_s - \kappa_f)}{\kappa_s + 2\kappa_f + 2\phi(\kappa_s - \kappa_f)}\right] \quad (6)$$

$$\mu_{nf} = \frac{\mu_f}{(1-\phi)^{2.5}} \quad (7)$$

$$(\rho C_p)_{nf} = (1-\phi)(\rho C_p)_f + \phi(\rho C_p)_s \quad (8)$$

$$\alpha_{nf} = \frac{\kappa_{nf}}{(\rho C_p)_{nf}} \quad (9)$$

Eq. (1) to Eq. (3) is transformed using similarity functions, the stream function are

$$\left.\begin{aligned} \psi = \sqrt{c\cdot\nu_f}\cdot f(\eta)\cdot x, \eta = \sqrt{\frac{c}{\nu_f}}\cdot y, \\ (T_w - T_\infty)\,\theta(\eta) = T - T_\infty \end{aligned}\right\} \quad (10)$$

$$\theta_w = \frac{T_w}{T_\infty} \quad (11)$$

Defining the stream function ψ that is, (u) = ψ_y,

(v) = -ψ_x, which satisfies the Eq. (1)and Eq. (5) to Eq. (9) are substituted into Eq. (2), Eq. (3) and Eq. (4), we get following no-linear ODE:

$$\left.\begin{aligned} f''' + ((1-\phi)^{2.5}M + K)\left(\frac{a}{c} - f'\right) + (1-\phi)^{2.5} \\ \left(1 - \phi + \phi\frac{\rho_s}{\rho_f}\right)\left(\frac{a^2}{c^2} + ff'' - f'^2 + \gamma\theta\right) = 0 \end{aligned}\right\} \quad (12)$$

$$\left.\begin{aligned} \theta'' + \frac{Pr}{\left(\frac{\kappa_{nf}}{\kappa_f} + N(1+(\theta_w-1)\theta)^3\right)}\cdot \\ \left[\begin{aligned} &\frac{3N}{Pr}\cdot(\theta_w - 1)(1+(\theta_w-1)\theta)^2\theta'^2 + \\ &\left(1 - \phi + \phi\frac{(\rho C_p)_s}{(\rho C_p)_f}\right)(F\theta' - 2F'\theta) + \lambda\theta \\ &+ \frac{Ec}{(1-\phi)^{2.5}}\theta' \end{aligned}\right] = 0 \end{aligned}\right\} \quad (13)$$

Boundary conditions for stretching and shrinking plate:

$$\left.\begin{aligned} f = S, f' = 1, \theta = 1 \text{ at } \eta = 0 \text{ (stretching)} \\ f = S, f' = -1, \theta = 1 \text{ at } \eta = 0 \text{ (shrinking)} \\ f' \to \frac{a}{c}, \theta \to 0, \ \eta \to \infty \end{aligned}\right\} \text{ as } y=0; \quad (14)$$

$Pr = \frac{v}{\alpha}$is the Prandtl number, $Ec = \frac{{u_w}^2}{C_p \Delta T}$ is the Eckerts number, $Gr = \frac{g\beta(T_w - T_\infty)x^3}{v^2}$ is the Grashof number, $\gamma = \frac{Gr}{Re^2}$ is the Buoyancy parameter, $S = -\frac{v_w}{\sqrt{cv_f}}$ is the injection parameter, $\lambda = \frac{Q_0 v_f}{c\kappa_{nf}}$ is the heat source/sink, $K = \frac{v_f}{cK_1}$ is the porous parameter, $N = \frac{16\sigma^* {T_f}^3}{3k_f K^*}$ is the thermal radiation parameter and $M = \frac{\sigma B_0^2}{\rho_f c}$ is the magnetic parameter.

For validating the results obtained from MAPLE 18 software, the values for the parameters as given in previously presented journals by Mahapatraand Gupta (2002); Hamad and Pop (2010) and Pal *et al*. (2014) are given in MAPLE 18 software to obtain heat transfer rate values and velocity profiles. From Table-2, the dimensionless heat transfer rates obtained from MAPLE 18 software is in agreement with previously published journals by Mahapatraand Gupta (2002) and Hamad and Pop (2010). From Figure-2 and Figure-3, the velocity profiles obtained in MAPLE 18 software is in perfect correlation with that of Pal *et al*. (2014) results.

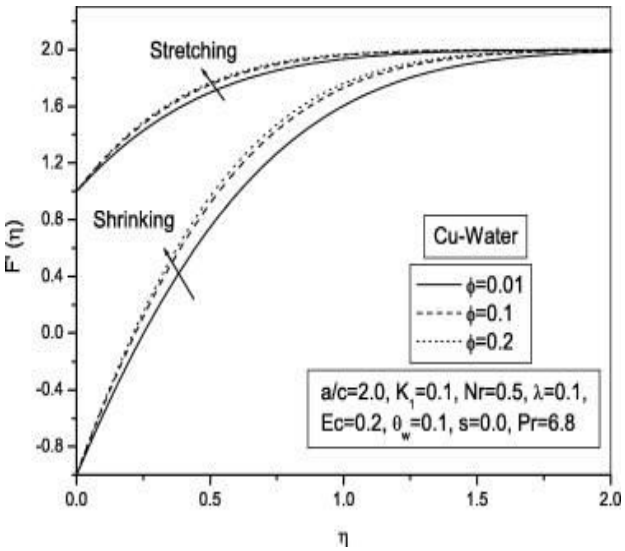

Figure-2. Nanoparticle volume fraction effect on copper nanofluid Pal *et al*. (2014).

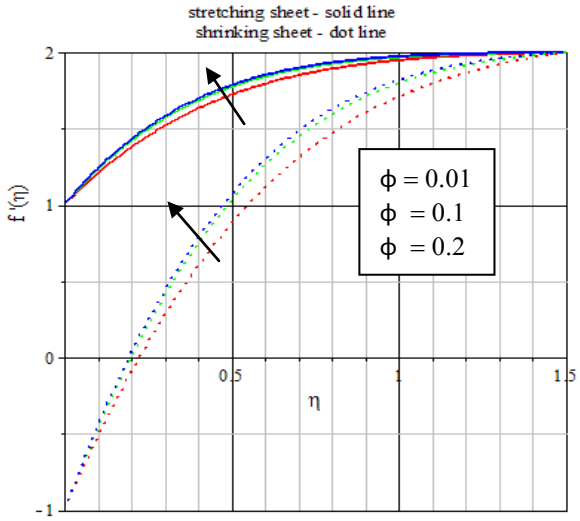

Figure-3. Nanoparticle volume fraction effect on copper nanofluid (MAPLE 18 software).

Table-2. Comparison of –θ'(0) obtained from MAPLE software with published works for stretching plate.

Pr	a/c	Mahapatra and Gupta (2002)	Hamad and Pop (2010)	Present results
1	**0.1**	**0.625**	**0.6216**	**0.62537**
	1	0.796	0.8001	0.79967
	2	1.124	1.1221	1.12375
1.5	0.1	0.797	0.7952	0.79500
	1	0.974	0.7952	0.79503
	2	1.341	1.3419	1.34095

RESULT AND DISCUSSIONS

In the presence of injection over the plate with constant Grashof number, profile for different values of magnetic strength (M) are seen in Figure-4 and Figure-5. Whenever an electrically conducting fluid is influenced by magnetic field a force acts in the opposite direction to the flow of fluid, opposing the motion of the nanofluid and

tends to increase the temperature profile. Velocity profiles decrease for increasing values of M.

In Figure-4, the behaviour of velocity profiles of nanofluid proves that by increasing the values of M, which is directly proportional to the magnitude of Lorentz force and as the Lorentz force increases, it opposes the fluid and decreases the velocity profiles. In Figure-5, the difference between temperature profiles is very less in both stretching and shrinking plates in the presence of injection. Temperature profiles of stretching has no significant changes when the flow is near to thermal boundary layer. Beyond $\eta = 0.6$, the temperature increases for stretching plates. In case of shrinking plates, temperature profiles decreases for increasing values of M. Beyond $\eta = 1$, there is an increase in temperature for increasing values of M.

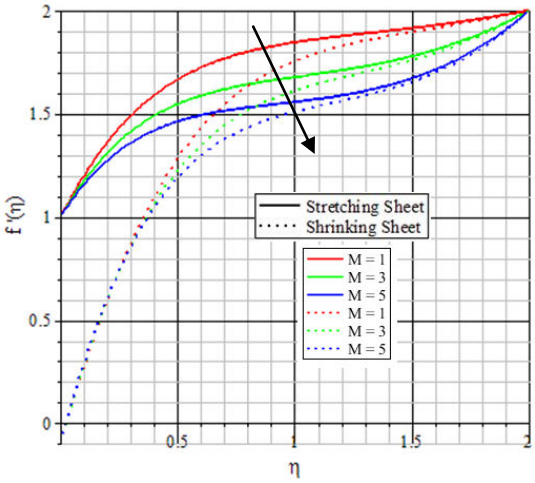

Figure-4. Magnetic field effects on velocity profiles of Cu-fresh water.

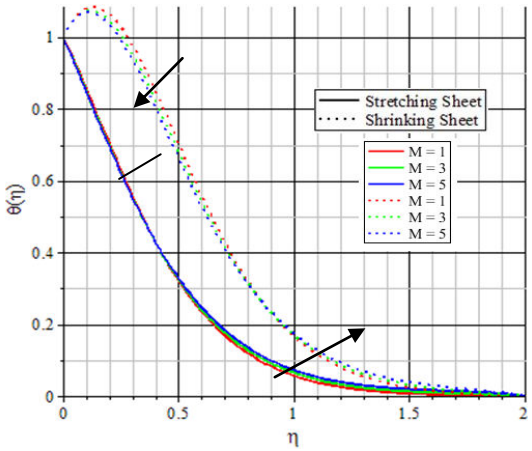

Figure-5. Magnetic field effects on temperature profiles of Cu-fresh water

In Figure-6, both stretching and shrinking plate shows increased velocity for higher Grashof number. In Figure-7, the temperature profiles for shrinking plate shows an interesting change. In the presence of uniform injection, it is predict that the temperature profiles attain peak at $\eta = 0.1$ and drastically reduces to zero as $\eta = 1.75$ for shrinking plate.

Figure-7, for shrinking plate, in the range $0 < \eta < 0.37$, it is observed that the temperature of the nanofluid increases with increase of Grashof number whereas $\eta \geq 0.75$, temperature decreases with increase in Grashof number. For stretching plate, since having higher velocity initially than the shrinking plate there is no peak formation in temperature profile. There is no significant change in temperature profiles but beyond $\eta = 0.42$, the temperature profile decreases with increase of Grashof number for stretching plate. The buoyancy effect has caused the peak formation in the presence of shrinking plate.

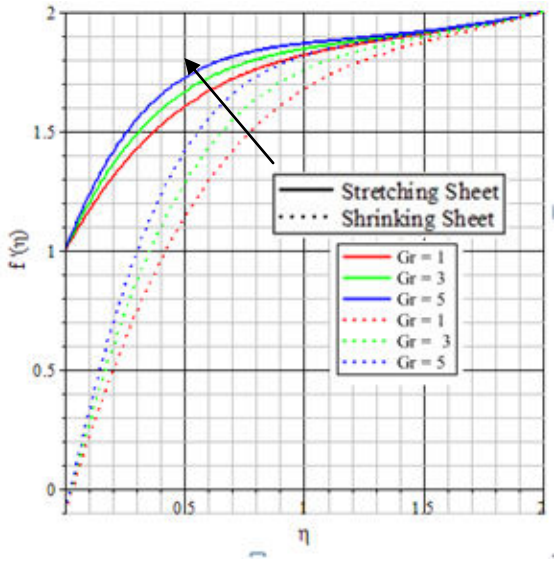

Figure-6. Grashof number effects on velocity profiles of Cu-fresh water.

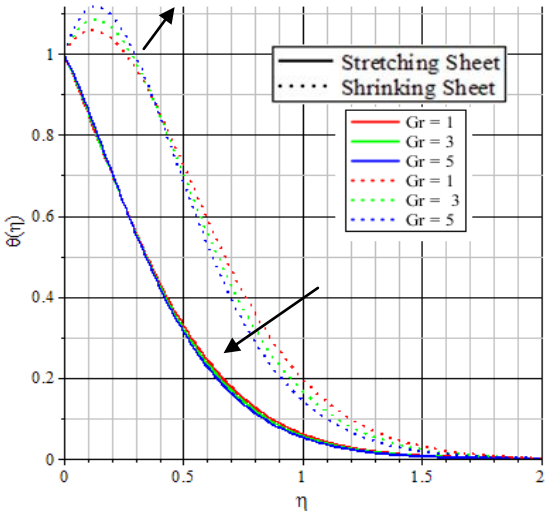

Figure-7. Grashof number effects on temperature profiles of Cu-fresh water.

Figure-8 and Figure-9, shows interesting results as the velocity and temperature decreases with increase in heat sink parameter with uniform injection. Difference in velocity profiles is very low in both shrinking and

stretching plates. In Figure-9, the presence of heat sink in the boundary layer causes the temperature of the fluid to decrease. This is due to fact that heat sink absorbs energy. There is a peak formation in temperature in case of shrinking plate. It is interesting to observe that the temperature profile for shrinking plate is more than the temperature profile for the stretching plate.

Effects of heat source on velocity and temperature distribution for stretching and shrinking plate along with the influence of injection of the plate are shown in Figure-10 and Figure-11. In Figure10, velocity increases for increasing values of heat source. Velocity gradient beyond $\eta = 1$ is very less for both stretching and shrinking plates. Heat source generates energy which causes the temperature of the fluid to increase in the Cu-fresh water boundary layer for stretching and shrinking plate.

In Figure-11, temperature profiles for shrinking plates is greater than the stretching plates. In case of shrinking plates, for all values of heat source, there is a peak formation in temperature profile. In case of stretching plate, it is interesting to note that, for high values of heat source, there is remarkable rise in temperature profiles. Increasing the heat source parameter has the tendency to increase the thermal state of the copper nanofluid. The explanation for these behaviour are due to the combined effects of the strength of convective radiation.

From Figure-12 and Figure-13, it is clearly visible that increase in nanoparticle volume concentration (ϕ), increases both velocity profiles and temperature profiles in the presence of shrinking as well as stretching plates. The concentration of nanoparticles in base fluid influences the velocity of the base fluid (fresh water).

In Figure-13, temperature profile in the presence of shrinking plate initially increases and goes to a peak at $\eta = 0.1$ and gradually decreases to zero. In addition, the results elucidate that the nanofluid heat transfer rate increases with an increase in the ϕ. There is no huge difference in temperature profiles for increasing ϕ values. It means that, efficient temperature profiles can be obtained with low nanoparticle volume concentration.

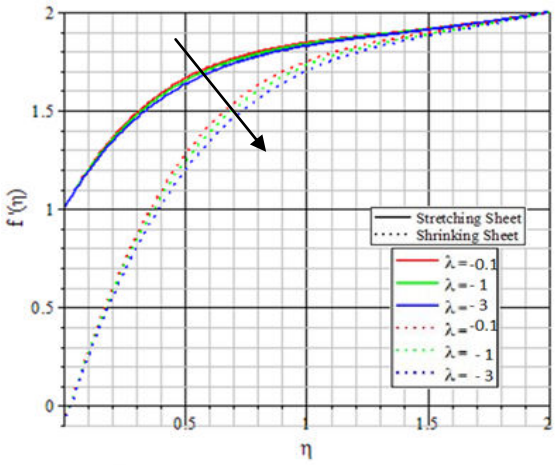

Figure-8. Heat sink effects on velocity profiles of Cu-fresh water.

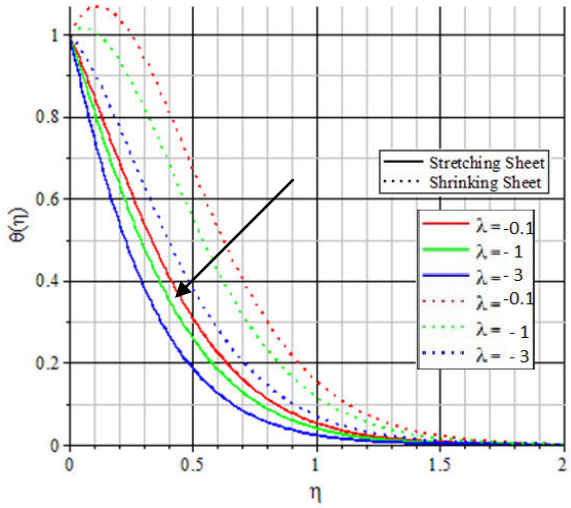

Figure-9. Heat sink effects on temperature profiles of Cu-fresh water.

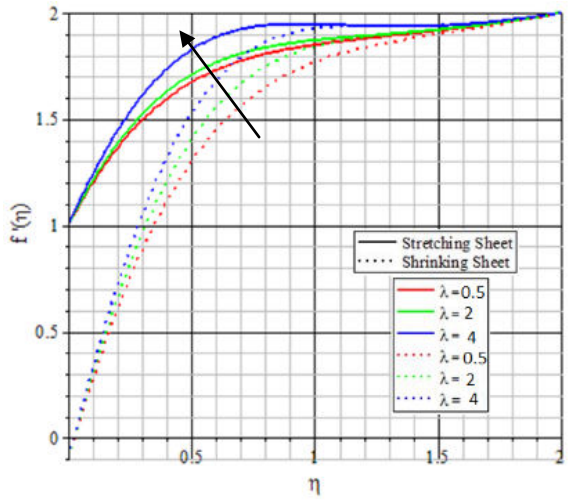

Figure-10. Heat source effects on velocity profiles of Cu-fresh water.

Figure-14 and Figure-15, shows the effect of thermal radiation in the presence of uniform injection velocity. Velocity distributions is similar in case of shrinking and as well as stretching. In Figure-15, for increasing thermal radiation (N), temperature profiles of both shrinking plate and stretching plate decreases near the thermal boundary layer and when the nanofluid moves away from the influence of boundary layer, the temperature profile increases.

This is because the large values of N correspond to an increased influence of conduction over radiation that reduces the buoyancy force and increasing the thickness of the thermal boundary layer, despite of improved thermal conductivity for specific volume concentration of copper nanoparticles. In Figure-15, nanofluid flow over shrinking plate forms a peak in temperature near the boundary layer. Temperature profiles of shrinking plates are higher than that of temperature profiles of stretching plate.

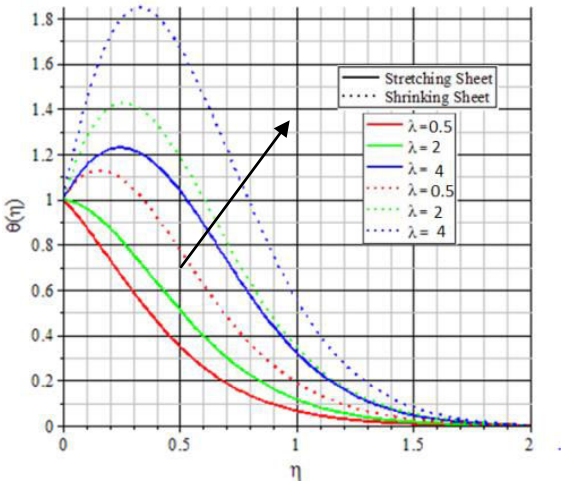

Figure-11. Heat source effects on temperature profiles of Cu-fresh water.

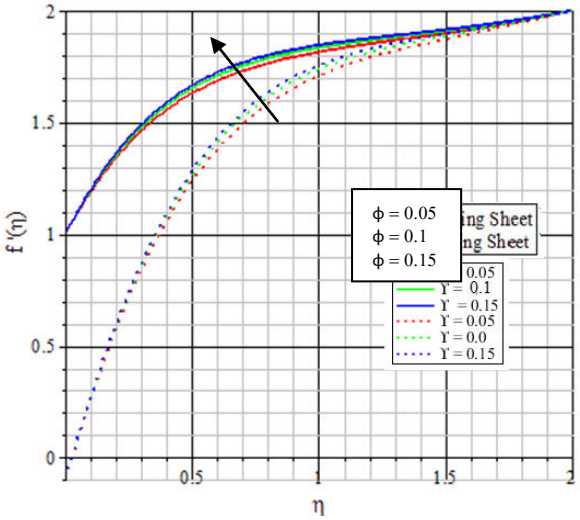

Figure-12. Nanoparticle volume fraction effects on velocity profiles of Cu-fresh water.

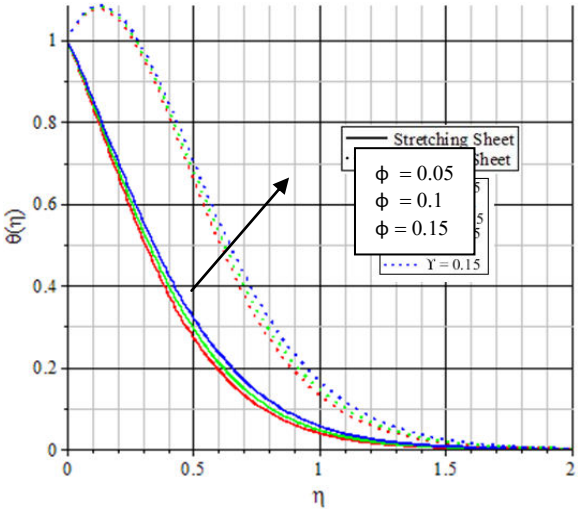

Figure-13. Nanoparticle volume fraction effects on temperature profiles of Cu-fresh water.

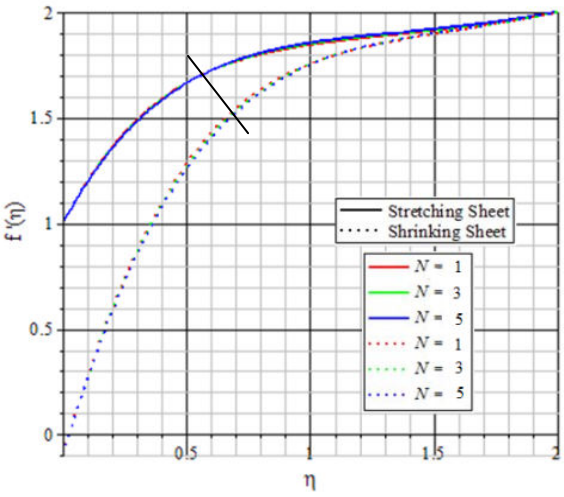

Figure-14. Thermal radiation effects on velocity profiles of Cu-fresh water.

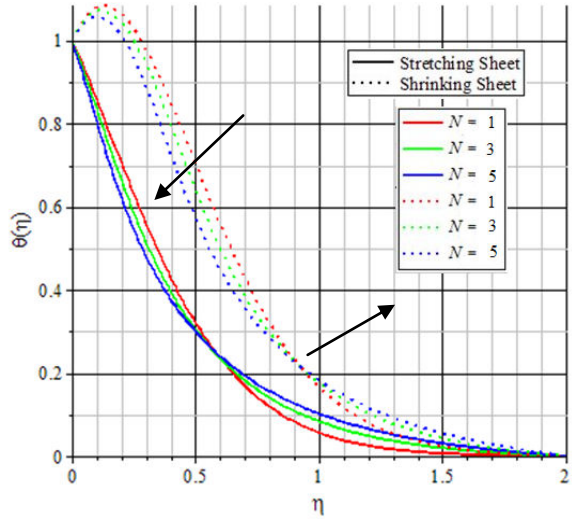

Figure-15. Thermal radiation effects on temperature profiles of Cu-fresh water.

Figure-16, by increasing the porous parameter (K) of the plates, the velocity increases for shrinking as well as stretching plates. The order of magnitude variation of the velocity profiles for different values of K is high in case of shrinking plate than the stretching plate. The velocity gradient is low beyond $\eta = 1$ for both shrinking and stretching plate.

In Figure-17, the temperature of the nanofluid increases to a peak value and reduces to zero as $\eta = 1.4$ for shrinking plate whereas outside $\eta = 0.3$, there is decrease in temperature for increase in porous parameter in shrinking plate. This is because, higher the porosity parameter, higher the velocity as fluid can easily flow through the plate. Temperature profiles of shrinking plates is high than stretching plate. Temperature profiles of shrinking and stretching plates tends to zero at $\eta = 1.9$ and $\eta = 1.7$ respectively.

In Figure-18 and Figure-19, depicts the influence of the injection parameter (S) on the velocity, temperature profiles in the boundary layer. In Figure-18, with the

increase in the value of injection velocity (S < 0), the velocity profiles of the Cu-fresh water nanofluid increases. The reason for such behavior is that in case of injection, fluid is pushed towards the wall and reduces buoyancy force which acts to oppose the fluid, because of high influence of Brownian motion.

In Figure-19, the temperature θ(η) in boundary layer increases with the decreasing injection parameter (S<0). The presence of injection at wall, decreases the velocity boundary layer thickness but increases the thermal boundary layers thickness. In the presence of shrinking plate, a peak formation is seen at η=0.15. Temperature profile is higher in the presence of shrinking plate than the presence of stretching plate.

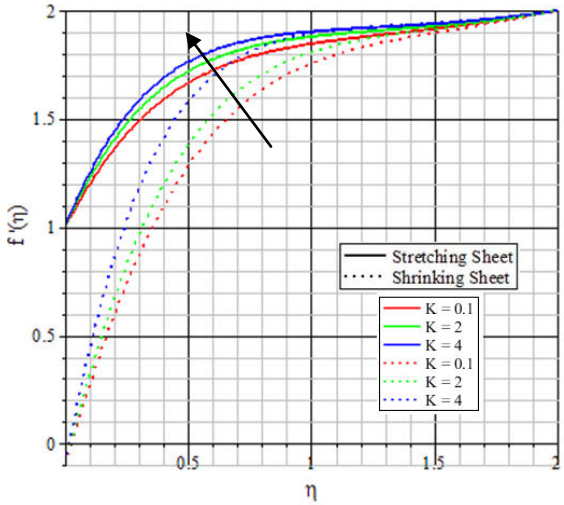

Figure-16. Porous parameter effects on velocity profiles of Cu-fresh water.

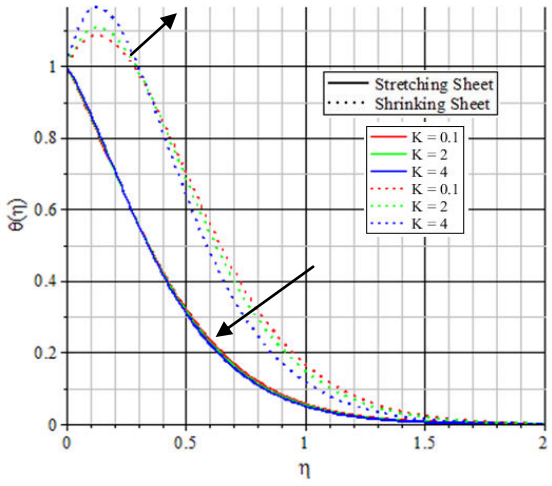

Figure-17. Porous parameter effects on temperature profiles of Cu-fresh water.

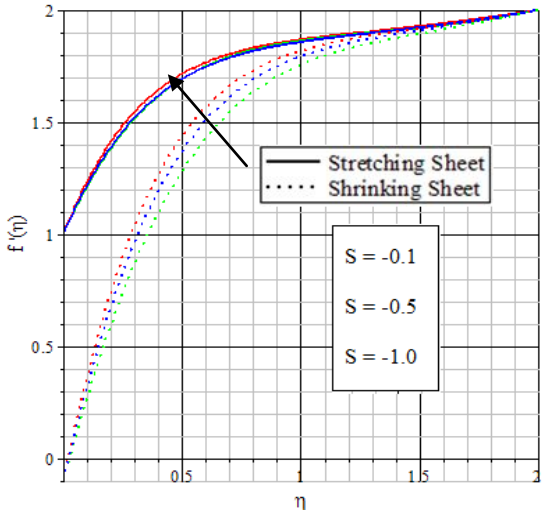

Figure-18. Injection parameter effects on velocity profiles of Cu-fresh water.

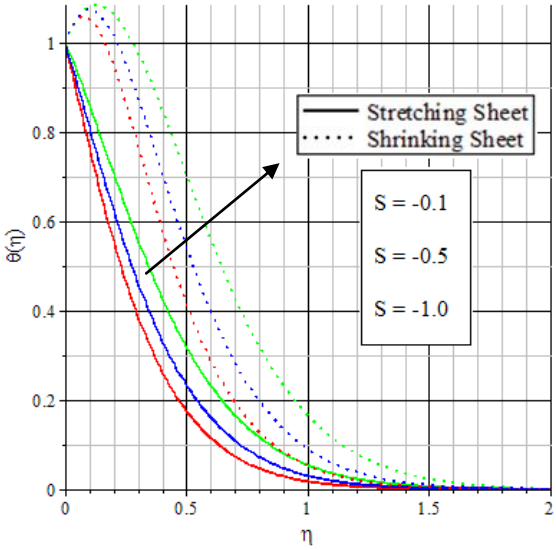

Figure-19. Injection parameter effects on temperature profiles of Cu-fresh water.

CONCLUSIONS

In this investigation, we have considered effects of injection, magnetic strength and Grashof number for 2-D stagnation-point flow over a porous medium considering nanofluids. Following conclusions are drawn from the present study:

1. In the presence of injection, it is significant to note that the temperature profile for shrinking plate is higher than stretching plate for copper nanofluids (Cu–fresh water). It implies that when the volume fraction of copper nanofluids in the presence of magnetic field, the thermal boundary layer thickness increases.
2. In the presence of copper nanofluid, the temperature of the fluid is uniform for stretching plate and decreases for shrinking plate with increase of magnetic strength. These results clearly demonstrate

that the magnetic field can be used as a means of controlling the flow and heat transfer characteristics. The result agrees with the expectations, since magnetic field exerts retarding force on the natural convection flow.

3. Due to injection of the plate, it is note that the temperature profiles for shrinking plate plays a important role compared to that of stretching plate for increasing thermal radiation. This is due to the fact that the large values the influence of conduction over radiation thereby reducing the buoyancy force and size of thermal boundary layer, despite of improved thermal conductivity for specific volume concentration of copper nanoparticles.
4. It is interesting to note that the temperature of the fluid gradually decreases only when the strength of injection parameter higher than the magnetic strength in the presence of Cu-water for shrinking plate because the copper (Cu) has high thermal conductivity.
5. The temperature profiles for shrinking plate is more than stretching plate and peak temperature is observed only in shrinking plate.
6. Increasing the porosity tends to decelerate the temperature in both shrinking and stretching plates.

Hence the nanoparticles may significantly increase the thermal conductivity heat transfer capabilities of fluids.

NOMENCLATURE

a,c	Constant (+ve)
B_0	Magnetic field strength
Cp_s	Specify heat of solid
Cp_f	Specific heat of fluid
Cp_{nf}	Specific heat of nanofluids
Cu	Copper nanoparticle
Ec	Eckert number
$f'(\eta)$	Dimensionless velocity
Gr	Grashof number
g	Gravitational force
K	Porous parameter
K_1	Permeability of the porous medium (m^2)
K^*	Mean spectral absorption coefficient (m^{-1})
M	Magnetic strength parameter ($Nm\ \Omega^{-1}A^{-2}\ s^{-1}$)
MHD	Magnetohydrodynamics
N	Thermal radiation parameter (s^3m^{-2})
ODE	Ordinary differential equations
PDE	Partial differential equations
Pr	Prandtl number
Q_o	Dimensional heat generation/absorption coefficient ($kgm^{-1}s^{-3}K^{-1}$)
Re	Reynolds number
S	Injection velocity parameter
T_f	Fluid Temperature
T_∞	Free stream temperature
T_w	Wall temperature
u, v	Velocity components in x,*y*-directions respectively
u_w	Stretching or shrinking surface velocity
v_w	Injection velocity
U	Free stream velocity of the nanofluid
2-D	Two-dimensional

Greek symbols

α_{nf}	T hermal diffusivity of the nanofluid
α_f	Fluid thermal diffusivity
β	Thermal expansion coefficient
γ	Buoyancy parameter
η	Similarity variable
$\theta(\eta)$	Dimensionless temperature of the fluid
θ_w	Wall temperature excess ratio parameter
$\theta'(\eta)$	Dimensionless heat transfer rate
κ	Thermal conductivity
κ_f	Thermal conductivity of the fluid
κ_{nf}	Effective thermal conductivity of the nanofluid
κ_s	Thermal conductivity of solid
λ	Heat sink/source parameter
μ_f	Dynamic viscosity of the fluid
μ_{nf}	Effective dynamic viscosity of the nanofluid
ρ_f	Density of fluid
ρ_{nf}	Effective density of the nanofluid
ρ_s	Density of solid
$(\rho C_p)_f$	Heat capacitance of fluid
$(\rho Cp)_{nf}$	Heat capacitance of nanofluid
$(\rho C_p)_s$	Heat capacitance of solid
σ	Electrical conductivity
σ^*	Stefan–Boltzmann constant
ϕ	Nanoparticles volume fraction
ψ	Stream function

Superscripts

Differentiate with respect to x, y and η correspondingly

Subscripts

f	Fluid
nf	Nanofluid
s	Solid

ACKNOWLEDGEMENT

The work was partly supported by Universiti Tun Hussein Onn Malaysia, Johor, Malaysia, under the Short Term Grant Scheme Vot.no. 1289.

REFERENCES

[1] Buongiorno, J., "Convective transport in nanofluids", Journal of Heat Transfer, vol. 128, (2006), pp. 240-250.

[2] Choi, S., "Enhancing thermal conductivity of fluids with nanoparticle, development and applications of non-Newtonian flow", ASME FED, 231/MD vol. 66, (1995), pp. 99-105.

[3] Eastman, J.A., Choi, S.U.S., Li, S., Yu, W. and Thompson, L.J., "Anomalously increased Effective thermal conductivity of ethylene glycol-based nanofluids containing copper nanoparticles", Applied Physics Letter, vol. 78 no. 6, (2001), pp. 718-720.

[4] Hamad, M.A.A. and Ferdows, M., "Similarity solution of boundary layer stagnation-point flow towards a heated porous stretching sheet saturated with a nanofluid with heat absorption/ generation and suction/blowing: a lie group analysis", Communications in Nonlinear Science Numerical Simulation, vol. 17, (2011),pp. 132–140.

[5] Hamad, M.A.A. and Pop, I., "Scaling transformations for boundary layer flow near the stagnation-point on a heated permeable stretching surface in a porous medium saturated with a nanofluid and heat generation/absorption effects", Transport in Porous Medium, vol. 87, (2010), pp. 25-39.

[6] Ibrahim, W., Shankar, B. and Nandeppanavar, M.M., "MHD stagnation point flow and heat transfer due to nanofluid towards a stretching sheet", International Journal of Heat and Mass Transfer, vol. 56, (2013), pp. 1-9.

[7] Ishak, A. and Nazar, R., "Uniform suction/blowing effect on flow and heat transfer due to a stretching cylinder", Applied Mathematical Modelling, vol. 32, no. 10, (2008), pp. 2059–2066.

[8] Khan, W.A. and Pop, I. Boundary-layer flow of a nanofluid past a stretching sheet, International Journal of Heat and Mass Transfer, vol. 53, (2010), pp. 2477-2483.

[9] Kuznetsov, A.V. and Nield, D.A., "Natural convective boundary layer flow of a nanofluid past a vertical plate", International Journal of Thermal Science, vol. 49, (2010), pp. 243-247.

[10] Mahapatra, T.R. and Gupta, A.S. "Magnetohydrodynamics stagnation-point flow towards a stretching surface", Acta Mechanica, vol. 152, no.1-4, (2001), pp. 191-196.

[11] Mahapatra, T.R. and Gupta, A.S. "Heat transfer in stagnation-point flow towards a stretching sheet", Heat Mass Transfer, vol. 38, (2002), pp. 517-521.

[12] Nazar, R., Jaradat, M., Arifin, M. and Pop, I., "Stagnation-point flow past a shrinking sheet in a nanofluid", Central European Journal of Physics, vol. 9, no. 5, (2011), pp.1195–1202.

[13] Nield, D.A. and Kuznetsov, A.V., "The Cheng-Minkowycz problem for natural convective boundary layer flow in a porous medium saturated by a noanofluid", International Journal of Heat Mass Transfer. vol. 52, (2009), pp. 5792–5795.

[14] Oztop, H. F. and Abu-Nada, E., "Numerical study of natural convection in partially heated rectangular enclosures filled with nanofluids", International Journal of Heat Fluid Flow, vol. 29, (2008), pp. 1326-1336.

[15] Pal, D., Mandal, G. and Vajravelu, K., "Flow and heat transfer of nanofluids at a stagnation point flow over a stretching/shrinking surface in a porous medium with thermal radiation", Applied Mathematics and Computation, vol. 238, (2014), pp. 208-224.

[16] Wang, X. and Mujumdar, A.S.,"A review on nanofluids-Part I: Theoretical and numerical investigation", Brazilian Journal of Chemical Engineering, vol. 25, no. 4,(2008), pp. 613-630.